Label-Free Electrophoretic Mobility Shift Assay (EMSA) for Measuring Dissociation Constants of Protein-RNA Complexes

Minguk Seo,[1] Li Lei,[1] and Martin Egli[1,2]

[1]Department of Biochemistry, School of Medicine, Vanderbilt University, Nashville, Tennessee
[2]Corresponding author: *martin.egli@vanderbilt.edu*

The electrophoretic mobility shift assay (EMSA) is a well-established method to detect formation of complexes between proteins and nucleic acids and to determine, among other parameters, equilibrium constants for the interaction. Mixtures of protein and nucleic acid solutions of various ratios are analyzed via polyacrylamide gel electrophoresis (PAGE) under native conditions. In general, protein–nucleic acid complexes will migrate more slowly than the free nucleic acid. From the distributions of the nucleic acid components in the observed bands in individual gel lanes, quantitative parameters such as the dissociation constant (K_d) of the interaction can be measured. This article describes a simple and rapid EMSA that relies either on precast commercial or handcast polyacrylamide gels and uses unlabeled protein and nucleic acid. Nucleic acids are instead detected with SYBR Gold stain and band intensities established with a standard gel imaging system. We used this protocol specifically to determine K_d values for complexes between the PAZ domain of Argonaute 2 (Ago2) enzyme and native and chemically modified RNA oligonucleotides. EMSA-based equilibrium constants are compared to those determined with isothermal titration calorimetry (ITC). Advantages and limitations of this simple EMSA are discussed by comparing it to other techniques used for determination of equilibrium constants of protein-RNA interactions, and a troubleshooting guide is provided.

Keywords: Ago2 • electrophoresis • equilibrium constant • protein–nucleic acid interaction • RNA

How to cite this article:
Seo, M., Lei, L., & Egli, M. (2019). Label-free electrophoretic mobility shift assay (EMSA) for measuring dissociation constants of protein-RNA complexes. *Current Protocols in Nucleic Acid Chemistry*, *76,* e70. doi: 10.1002/cpnc.70

BASIC PROTOCOL

Nucleic acid–protein interactions are ubiquitous and absolutely essential in biological information transfer, including replication, transcription, repair, and RNA metabolism (Cusack et al., 2017). Gel electrophoresis using polyacrylamide gels (PAGE; Andrus & Kuimelis, 2001a) and the electrophoretic mobility shift assay (EMSA) remain important and are widely used approaches for detecting nucleic acid–protein interactions and determining the stability of individual complexes (Alves & Cunha, 2012; Chen, 2011; Fried, 1989; Hellman & Fried, 2007). This protocol details the steps for establishing the equilibrium dissociation constant K_d of an RNA-protein complex by EMSA. Solutions of RNA and protein are mixed in different ratios, and the

CURRENT PROTOCOLS
A Wiley Brand

Current Protocols in Nucleic Acid Chemistry e70, Volume 76
Published in Wiley Online Library (wileyonlinelibrary.com).
doi: 10.1002/cpnc.70

binding reactions are then separated by non-denaturing PAGE (*https://tools.thermofisher.com/content/sfs/brochures/1601945-Protein-Interactions-Handbook.pdf*). In general, a protein-RNA complex will migrate more slowly through the gel matrix relative to the RNA alone, thus causing a shift on the gel (e.g., Yang et al., 1999). Individual bands can be visualized by end-labeling the RNA radioactively (^{32}P) or by using fluorescent or chemiluminescent probes in combination with a gel imager. However, in our assay, we have used non-labeled RNA together with the SYBR Gold stain (Tuma et al., 1999) for detecting and quantifying bands. From the distribution of the RNA component among the protein-RNA and RNA bands in individual lanes on the gel, one can determine the equilibrium dissociation constant K_d of the complex in a straightforward manner. An approximate value for the equilibrium constant can be obtained by finding the concentration of protein at which roughly half the nucleic acid component is bound and half remains free. A more precise way to determine K_d is to plot individual fractions of the nucleic acid bound in each reaction versus the concentration of protein and then perform a nonlinear regression (Heffler, Walters, & Kugel, 2012) using free or commercially available software.

Human Argonaute 2 (Ago2) is an 859–amino acid protein that lies at the heart of the RNA-induced silencing complex (RISC; Sheu-Gruttadauria & MacRae, 2017). The protein binds small interfering RNA (siRNA) duplexes consisting of 21mer guide (antisense) and passenger (sense) strands with 3′-terminal dinucleotide overhangs. Ago2 contains multiple domains, including the MID (binds 5′-end of guide siRNA), PIWI (harbors the endonuclease active site), PAZ (binds 3′-end of guide siRNA), and two linkage domains. The passenger strand is eventually cleaved or discarded and the target RNA loaded into Ago2 opposite the guide strand, resulting in cleavage of the former by the PIWI domain via a dual-metal ion mechanism (Watts & Corey, 2012; Wilson & Doudna, 2013). RISC contains other Ago proteins besides Ago2 (i.e., Ago1, Ago3, and Ago4), and while all are associated with micro RNAs (miRNAs), only Ago2 exhibits endonuclease activity (Meister et al., 2004). Chemically modified siRNAs are widely explored as therapeutics for treatment of a range of diseases (Crooke, Witztum, Bennett, & Baker, 2018; Shen & Corey 2018). ONPATTRO (Patisiran) is a modified siRNA formulated in lipids and manufactured by Alnylam Pharmaceuticals Inc. (Cambridge, MA) that was approved by the US FDA in August of 2018 for the treatment of polyneuropathy of hereditary transthyretin-mediated amyloidosis in adults (Sheridan, 2017). The PAZ domain of Ago2 binds the last two nucleotides of guide siRNA and assists in separating guide and passenger siRNA (Elkayam et al., 2012; Ma, Ye, & Patel, 2004; Schirle & MacRae, 2012; Fig. 1). The identities of the 3′-overhanging nucleotides in the siRNA guide strand and their chemical modification affect the interaction with Ago2 PAZ and silencing activity (Alagia et al., 2018; Kandeel et al., 2014). We relied on the EMSA protocol presented here to determine equilibrium dissociation constants K_d of the interactions between native and chemically modified RNAs and the human Ago2 PAZ domain.

The following procedures outline the mixing of RNA and protein solutions of defined concentrations in various ratios to establish the binding reactions, the preparation of polyacrylamide gels to run EMSAs for analyzing protein-RNA binding, staining and imaging of gels to measure the intensities of individual bands and the distribution of RNA between the free and protein-bound forms, and the determination of K_d values using standard software to compute nonlinear regressions. However, neither the synthesis of RNA oligonucleotides nor the expression and purification of the Ago2 PAZ domain are described in detail. Briefly, RNAs were provided by Alnylam Pharmaceuticals Inc. (Cambridge, MA; native oligoribonucleotides) or AM Biotechnologies LLC (Houston, TX; 2′-*O*-Me/3′-phosphorodithioate [PS2; both non-bridging phosphate oxygen atoms replaced with sulfur] oligoribonucleotide, hereafter referred to as MS2-modified RNA).

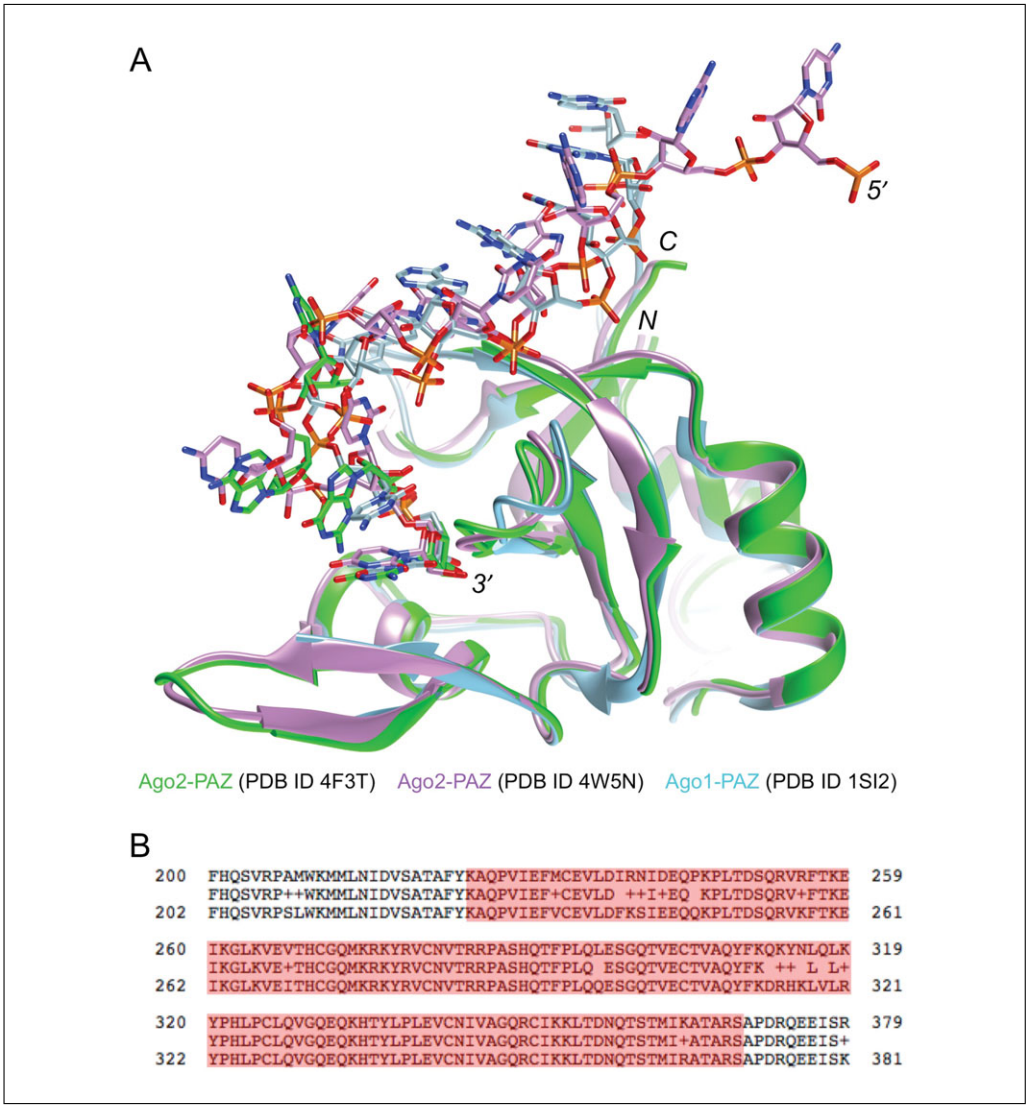

Figure 1 Overlay of crystal structures of human Ago1- and Ago2-PAZ in complex with RNA oligonucleotides (**A**) and alignment of the human Ago1 (top line) and Ago2 (bottom line) sequences (**B**). Only a portion of the 859 amino acids is included; the consensus sequence is shown in the middle line with PAZ domain residues highlighted: 225 to 369 (Ago1) and 227 to 371 (Ago2). The PAZ domain binds the 3′-end of guide siRNA. The models shown are from crystal structures of full-length Ago2 bound either to duplex RNA (Schirle & MacRae, 2012) or an miRNA single strand (Elkayam et al., 2012). In both cases, only PAZ domain residues 226 to 351 were included in the illustration. In both crystal structures, only portions of the 3′-half of the RNA guide strand were visible in the electron density. The third structure depicted is of a complex between a separately expressed human Ago1 PAZ domain (residues 224 to 349 were resolved in the electron density) and an RNA nonamer (Ma et al., 2004). Coordinates were retrieved from the Protein Data Bank (PDB; *https://www.rcsb.org/*; Berman et al., 2000), and the structural figure in (A) was generated with the program UCSF Chimera (Pettersen et al., 2004).

Native RNAs were synthesized by standard or adapted solid phase phosphoramidite synthesis, purified (Andrus & Kuimelis, 2001b) by high-performance liquid chromatography (HPLC; Sinha & Jung, 2015), and desalted (Andrus & Kuimelis, 2001c). Identities and purities of all oligonucleotides were confirmed by electrospray ionization mass spectrometry (ESI-MS) and ion-exchange HPLC (IEX-HPLC), respectively. The MS2-modified RNA was synthesized and purified as reported in Yang (2017). An expression system for human Ago2 PAZ (amino acids 227 to 371; Fig. 1B) was generated by gene synthesis (GenScript Inc.) and subcloning into the pHD116 plasmid. The plasmid was transformed into *E. coli* BL21 (DE3) Gold cells using standard procedures. After expression the

protein was first purified by nickel affinity chromatography and, following cleavage of the His_6 tag by PreScission protease (GE Healthcare), by ion exchange and gel filtration chromatography. The identity of the Ago2 PAZ domain was established by tryptic digestion in combination with MS analysis.

Materials

1% (w/v) agarose (see recipe)
5% (w/v) polyacrylamide gel solution (see recipe)
5× Tris/borate/EDTA (TBE) buffer (see recipe)
500 nM RNA(s) of interest (see Fig. 2 for sequences)
Nuclease-free water (e.g., Promega, cat. no. P119E-C)
Human Ago2 PAZ domain protein (see recipe)
1× binding buffer (see recipe)
Bromophenol blue dye
25 mg/mL Ficoll (e.g., Sigma-Aldrich, cat. no. 26873-85-8)
10,000× Sybr Gold (e.g., Invitrogen, cat. no. S11494)

Gel electrophoresis apparatus (e.g., Bio-Rad Mini-PROTEAN Tetra Cell System) containing:
  1.5-mm-thick mini gel glass plates
  Gel combs
  Electrophoresis unit
  Power supply
1.5-mL microcentrifuge tubes
Black cassettes
Gel imaging system (e.g., Bio-Rad ChemiDoc MP Imaging System)
Computer running image analysis software (e.g., ImageJ)

Prepare and pre-run gel

1. Make a 5% native TBE polyacrylamide gel by first assembling two 1.5-mm-thick glass gel plates (i.e., with clips), and set into the gel apparatus.
2. Seal the bottom of the gel plates with 1% agarose using a 1.0-mL micropipette.

   Be sure to pipette agarose on both sides of the gel plates to seal them as well.
3. Prepare 10 mL of 5% polyacrylamide gel solution (0.5× TBE).
4. Using a 1.0-mL micropipette, inject the polyacrylamide solution into the gel cast. Insert the comb into the assembled gel sandwich. Wait 1 hr to let the gel polymerize.

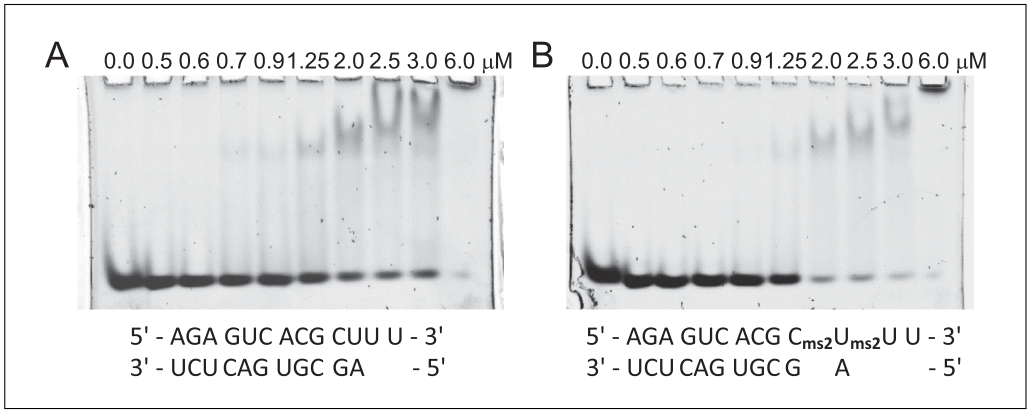

Figure 2 Gel images of binding reactions with various ratios between Ago2 PAZ and (**A**) native RNA and (**B**) MS2-modified RNA. RNA sequences are shown below the gels, and protein concentrations are shown above individual lanes. The RNA concentration was 250 nM.

Table 1 Sample Volumes and Concentrations of PAZ and RNA Needed for ESMA

Protein concentration (nM)	PAZ protein added (μL)	1× binding buffer added (μL)	RNA(s) of interest added (μL)
500	1.0 (10 μM stock)	9.0	10.0 (500 nM stock)
600	1.2	8.8	10.0
700	1.4	8.6	10.0
900	1.6	8.2	10.0
1250	2.5	7.5	10.0
2000	4.0	6.0	10.0
2500	5.0	5.0	10.0
3000	6.0	4.0	10.0
6000	3.0 (40 μM stock)	7.0	10.0

5. Prepare electrophoresis running buffer by diluting 100 mL of 5× TBE buffer with 900 mL sterile water to create 1 liter of 0.5× TBE.
6. Pre-run the polyacrylamide gel by submerging the cast gel in the running buffer from step 5, and run at 45 V to 60 V for 1 hr or until the current is stable.

Prepare sample and run and stain the gel

7. Prepare 100 μL of 500 nM RNA stock per gel in nuclease-free water, and dilute PAZ protein with 1× binding buffer to create two protein stock solutions, one of 10 μM concentration and the other of 40 μM concentration.
8. Allow the stock solutions prepared in step 7 to warm to room temperature, and then prepare nine human Ago2 PAZ protein and RNA binding mixtures in separate 1.5-mL microcentrifuge tubes according to Table 1. Create a control sample by mixing 10 μL RNA and 10 μL bromophenol blue dye. Incubate at room temperature for 30 min.
9. After the incubation is complete, add 2 μL Ficoll solution to each tube, including the control.
10. Load 20 μL of each sample into a well with the gel. Load the control sample into the first lane.
11. Run the gel at 40 to 70 V, 6 to 15 mA, for 1 hr or until the samples are roughly two-thirds down the gel (Fig. 2).
12. Add 5 μL of 10,000× Sybr Gold to 50 mL of 0.5× TBE buffer to create 50 mL of 1× Sybr Gold solution.
13. Stain each gel by submerging it in 50 mL of 1× Sybr Gold in a black cassette for 30 min.

    The Sybr Gold stain does not bind to the Ago2 PAZ domain.

14. Rinse gels with deionized water (optional).
15. Image gel using a gel imaging system (e.g., ChemiDoc MP Imaging System with a Blot/UV/Stain-Free Sample Tray; *http://www.bio-rad.com/en-us/product/chemidoc-mp-imaging-system?ID=NINJ8ZE8Z*; Fig. 2).
16. Calculate the binding affinity between the RNA and the protein by analyzing the gel images with ImageJ. See the Anticipated Results section for more details.

REAGENTS AND SOLUTIONS

Agarose, 1%

0.5 g agarose
50 mL 0.5× TBE buffer (see recipe)
Store at 4°C for up to 2 weeks

Ammonium persulfate (APS) solution, 10%

0.1 g APS (e.g., Bio-Rad, cat. no. 161-0700)
1 mL sterile water
Prepare freshly before use

Binding buffer, 1×

1 mL 10× binding buffer (see recipe)
2 mL 50% glycerol (e.g., RPI Corp., cat. no. 56-81-5)
7 mL sterile water
Store at 4°C for up to 2 weeks

Binding buffer, 10×

0.1 mM HEPES
1.5 M NaCl (e.g., Acros Organics, cat. no. 7647-14-5)
30 mM EDTA (e.g., Sigma-Aldrich, cat.no. 60-00-4)
10 mM DTT (e.g., Sigma-Aldrich, cat. no. 3483-12-3)
Store at 4°C for up to 2 weeks

Human Ago2 PAZ domain protein

180 μM PAZ protein
5 mM HEPES
100 mM KCl
10 mM DTT (e.g., Sigma-Aldrich, cat. no. 3483-12-3)
Store at −80°C for up to 1 year

Polyacrylamide gel solution, 5%

7.27 mL sterile water
1.66 mL 30% acrylamide/bis solution 37.5:1 (e.g., Bio-Rad, cat. no. 161-0158)
1.00 mL 5× TBE (see recipe)
70 mL 10% APS (see recipe)
3.5 mL tetramethylethylenediamine (TEMED; e.g., Bio-Rad, cat. no. 161-0800)
Prepare freshly before use

TBE buffer, 5×

1 liter water
54 g Tris base (e.g., RPI Corp., cat. no. 77-86-1)
27.5 g boric acid (e.g., RPI Corp., cat. no. 10043-35-3)
20 mL 0.5 M EDTA (e.g., Sigma-Aldrich, cat. no. 60-00-4), pH 8.0
Store at room temperature for up to 2 months

To prepare 0.5× TBE buffer, dilute 100 mL of 5× TBE buffer with 900 mL sterile water.

COMMENTARY

Background Information

There are multiple techniques for determining the equilibrium dissociation constant K_d of a protein–nucleic acid binding interaction besides the EMSA (Alves & Cunha, 2012; Chen, 2011; Fried, 1989; Heffler et al., 2012; Hellman & Fried, 2007). These include the filter-binding assay (Woodbury & von Hippel, 1983), fluorescence intensity (Teplova et al., 2000), chemical shift differences using

^{1}H–^{15}N heteronuclear single quantum coherence (HSQC) nuclear magnetic resonance (NMR) titration experiments (Frank, Hauver, Sonenberg, & Bushan, 2012), surface plasmon resonance (SPR; Ma et al., 2004; McDonnell, 2001), acoustic measurements (Cooper & Whalen, 2005; Godber et al., 2005), biolayer interferometry (BLI; Lou, Egli, & Yang, 2016), microscale thermophoresis (MST; Mueller et al., 2017), and isothermal titration calorimetry (ITC; Rozners, Pilch, & Egli, 2015), among others.

The choice to use one method versus another may depend on the amount of material available, the particular environment in which the experiment is to be conducted (e.g., solution, chip, microfluidics, cell), whether labeling can be accomplished relatively easily and/or cheaply, or whether equipment that is needed with some of the above techniques is accessible to the investigator. Thus, EMSAs, spectroscopic approaches, and SPR require less material than filter-binding assays and ITC. An important consideration concerns the K_d limit, that is the upper end of the stability range for the complex between protein and nucleic acid of interest at which a particular technique still affords precise data. In this regard, EMSA, SPR, and BLI allow reliable measurements of interactions with K_d values of as low as 10^{-12} M (Jing & Bowser, 2011). This contrasts with the K_d limit for ITC that is around 10^{-8} to 10^{-9} M. However, ITC, despite this limitation and the need for relatively large amounts of material, offers the benefits of a solution environment and label-free binding partners; it is also the method of choice to establish precise thermodynamic parameters of a binding interaction (ΔH, ΔS, and ΔG; Rozners et al., 2015). Most of the alternative approaches that yield the K_d of an interaction require labeling of either protein or nucleic acid, such as ^{15}N (protein; NMR), ^{32}P (DNA or RNA; filter-binding assay, EMSA), biotinylation (DNA or RNA; SPR, BLI; Lou et al., 2016), or fluorescent probes (protein or nucleic acid; MST, EMSA; Jiang & Egli, 2011).

We opted to use EMSA with label-free oligoribonucleotides to determine the K_d of the interaction between human Ago2 PAZ and RNA. Advantages of this approach are speed, low cost, and the small amount of material needed. A familiar limitation lies in the environment (i.e., a gel matrix and not solution) that can potentially affect the binding reaction. The complex between PAZ domain and RNA is known to be of a 1:1 stoichiometry (Fig. 1A), but published data reveal somewhat divergent values for the stability of the complex. Thus, the K_d values for the interactions between Ago2 PAZ and mono- (e.g., UMP) and dinucleotides (e.g., UpUMP) varied between 10 and 60 μM based on ITC (Kandeel et al., 2014). In contrast, the K_d of the interaction between Ago1 PAZ and an 11mer/13mer RNA duplex with a 3′-terminal dinucleotide overhang (Fig. 2A) was reported to be 2.2 nM as determined by SPR (Ma et al., 2004; Ago1 and Ago2 PAZ have highly similar sequences; Fig. 1B). In order to verify the EMSA-based K_d values, we therefore decided to also conduct independent ITC experiments. The outcomes of the two approaches are discussed in the Anticipated Results section.

Critical Parameters and Troubleshooting

We have tested two types of polyacrylamide gels and varied their percentages.

(1) *TBE polyacrylamide gel*: We started from 15% and then continuously lowered the percentage to 12%, 10%, 8%, 5%, and finally to 3.5%, as gels of higher percentage polyacrylamide prevented the complex from getting into and migrating through the gel. However, a 3.5% gel turned out to be too frail to handle, and it also showed no significant improvement compared to the 5% gel in terms of the migration of the complex. Thus, a 5% gel was judged to be optimal in terms of structural integrity and migration of the complex, even at higher concentrations of PAZ protein.

(2) *Tris-glycine polyacrylamide gel*: We assayed binding reactions on 4% to 20%, 12%, 10%, and 7.5% gels. Although the complex band migrated through the gel, increasing the protein:RNA ratio did not result in reduced and increased intensity of the RNA and complex band, respectively, and such gels apparently do not constitute a suitable environment for the PAZ-RNA complex.

We also examined the effects of varying the pH (e.g., 1% TBE, pH 8.0, and 0.5% TBE, pH 7.6) and the addition of detergents (0.04% sodium cholate, 1/10 CMC; 0.008% Triton X-100, 1/2 CMC). However, detergents proved to be detrimental to the complex. Thus, a 0.5× TBE buffer for both gel and running buffer yielded much better results. We did not use Mg^{2+} or Ca^{2+} in the buffer, and neither was used for annealing the RNAs. We do not anticipate that the presence of these ions would have a significant effect. Moreover, neither ion is present in or near the binding pocket of the PAZ domain.

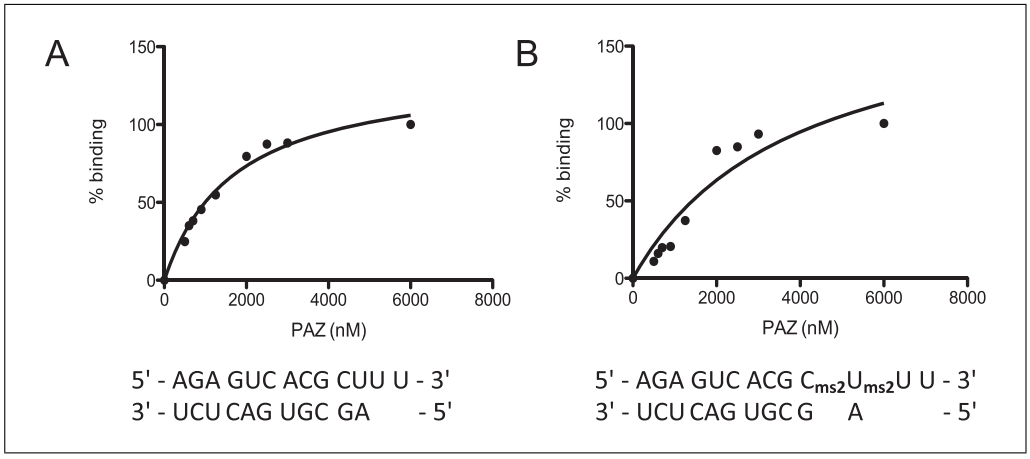

Figure 3 Nonlinear regressions for the PAZ complex with (**A**) native RNA and (**B**) modified RNA based on the gels depicted in Figure 2.

We observed that gel bands representing the PAZ-RNA complex tended to smear and that migration was limited at the highest ratio between protein and RNA. This issue may become exacerbated by the use of higher concentrations of protein and RNA owing to the lack of labels on the latter. However, the RNA bands were typically quite sharp, allowing reasonably precise density measurements even in cases where migration of the complex was limited or bands representing the complex were spread out.

For PAGE experiments one can of course use either precast or handcast gels. We have relied on commercial precast gels in some cases but have also poured our own gels. There are various systems on the market that facilitate hand pouring gels, (e.g., Sure Cast Gel Handcast System offered by Thermo Fisher; *https://www.thermofisher.com/us/en/home/life-science/protein-biology/protein-gel-electrophoresis/protein-gels/surecast-gel-handcast-system.html*).

Anticipated Results

To analyze the gel image obtained, the NIH program ImageJ was used (Schneider, Rasband, & Eliceiri, 2012). The program can be downloaded from the NIH website for free (*https://imagej.nih.gov/ij*). The image shown in Figure 2 was first inverted, and then the raw integrated density (RID) of each band was measured with ImageJ. ImageJ may not have the RID as a default setting. If that is the case, go to the "Analyze" tab, click "Set Measurements," check the "Integrated Density" box, and then click "OK." The results were then transferred into an Excel spreadsheet to perform the following calculations. Each RID was subtracted from the lowest RID, with the lowest RID being subtracted from itself resulting in zero. These values are the relative RIDs. Each relative RID was divided by the largest relative RID and then multiplied by 100, with the largest relative RID being divided by itself and then multiplied by 100, resulting in 100. These are the percentage RIDs. Finally, each percentage RID was subtracted from 100, resulting in the percentage of binding (i.e., complex formation, for each protein concentration).

These results then served as input for GraphPad Prism (version 5.00 for Mac; GraphPad Software, La Jolla, CA; *https://www.graphpad.com/*). Select the option that plots a single "Y" value for each data point, and press create. Enter the protein concentrations in the x-column, and enter the percent binding in the y-column. Label both columns. Next, click on the results tab, and select nonlinear regression (curve fit) under "XY analyses." Then select the equation that is labeled "one site–specific binding," which computes the K_d value (Fig. 3).

The K_d values obtained for the PAZ complexes with native and modified RNA are shown in Table 2.

Our EMSA is relatively simple, cheap, and quick. However, we wanted to determine if it also provided reasonably accurate data, keeping in mind the usual limitations of a gel-based assay. We therefore decided to compare the EMSA-based data to K_d values obtained from ITC experiments. These K_d values were 0.6 μM (PAZ complex with native RNA; Fig. 4A) and 1.9 μM (PAZ complex with modified RNA; Fig. 4B) and therefore quite similar to the EMSA data. Typically, one would carry out the EMSA in triplicate and then report average values.

Table 2 K_d Values Obtained for PAZ Complexes with Native and Modified RNA

RNA	K_d [μM], nonlinear fit
5′–AGA GUC ACG CUU U–3′ 3′–UCU CAG UGC GA–5′	1.7
5′–AGA GUC ACG $C_{ms2}U_{ms2}$U U–3′ 3′–UCU CAG UGC G A –5′	3.9

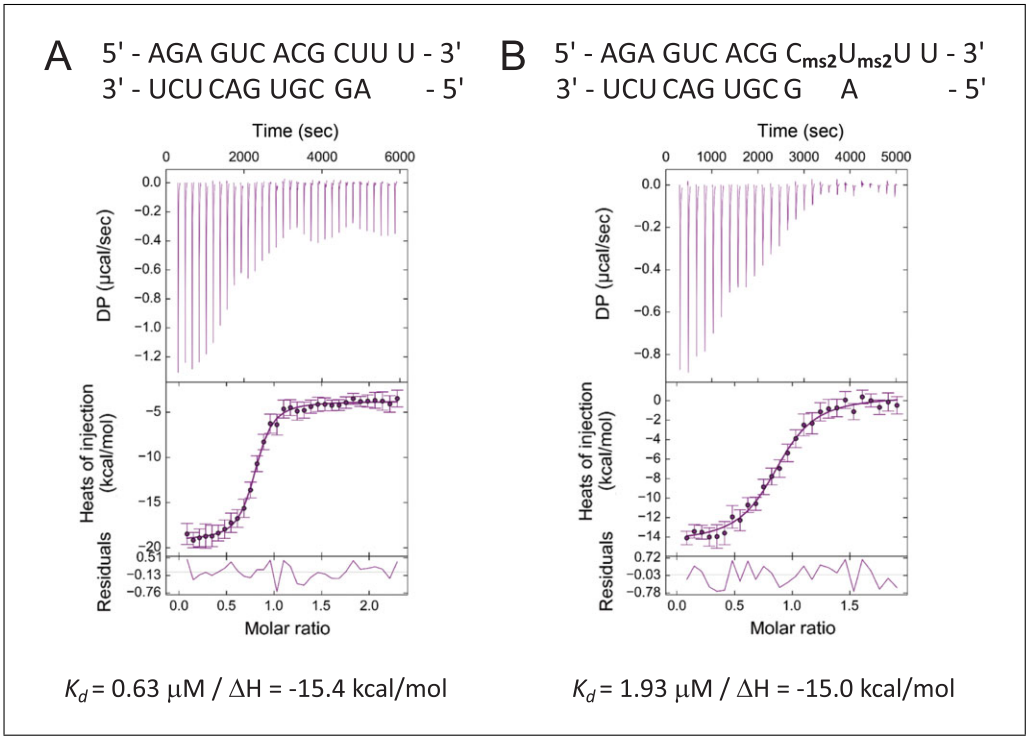

Figure 4 Results of isothermal titration calorimetry experiments for the PAZ complex with (**A**) native RNA and (**B**) modified RNA. The experiments were conducted under the following conditions: 56 μM Ago2 PAZ and 600 μM RNA in a buffer composed of 5 mM HEPES, pH 7.5, 150 mM KCl, 10% glycerol, and 10 mM DTT. RNA was added to the protein solution using 28 to 33 1.2-μL injections at 25°C. Note the 1:1 stoichiometry of the complexes, consistent with the structural models depicted in Figure 1A.

An earlier publication had reported a 2.2 nM K_d for the Ago1 PAZ complex with the same native RNA construct that was employed here and using SPR (Ma et al., 2004). However, we believe that this may be an overestimation of the tightness of binding between PAZ domain and RNA. For one, Ago1 and Ago2 PAZ have similar sequences (Fig. 1B), and it is unlikely that the former should exceed the latter in terms of its affinity for RNA by three orders of magnitude. In addition, the buried surface (binding interface, calculated with the program PRince; Barik, Mishra, & Bahadur, 2012; *http://www.facweb.iitkgp.ac.in/~rbahadur/prince/home.html*) in a complex between thrombin and an anti-thrombin RNA aptamer (Long, Long, White, & Sullenger, 2008; PDB ID 3DD2) that exhibits a K_d of 1 nM (Abeydeera et al., 2016), protein 719 Å^2, and RNA 790 Å^2 is much larger than that between Ago2 PAZ and the 3′-end of an RNA (complex with PDB ID 4F3T; Fig. 1A): protein 344 Å^2 and RNA 465 Å^2. However, it is of note that complexes can exhibit dramatically different stabilities as a consequence of a key interaction that leaves the buried surface essentially unchanged. Thus, replacement of a single phosphate (PO2) by a phosphorodithioate (PS2) moiety in RNA aptamers was reported to trigger a dramatic change in the dissociation constant of the complexes with their respective targets from about 1 nM to about 1 pM (anti-thrombin and anti-VEGF aptamers; Abeydeera et al., 2016).

Finally, the K_d values for complexes between PIWI protein PAZ domains and various RNAs based on ITC were recently reported to be between 2 and 34 μM (Tian, Simanshu, Ma, & Patel, 2011).

Time Considerations

The entire experiment, from pouring the gels to imaging and calculating the K_d value takes around 6 hr. Pouring, preparing, waiting for the gel to polymerize, and pre-running the gel can be accomplished in around 2 hr. Doing the calculations to prepare the individual samples, preparing the samples, loading the samples, and running the gel takes 2 to 3 hr. Finally, gel imaging, measuring band densities with ImageJ, and obtaining the K_d value using Prism takes another hour. With one gel apparatus, two gels can be run simultaneously, and thus K_d values for two complexes can be obtained on the same day.

Acknowledgments

We are grateful to Alnylam Pharmaceuticals Inc. for synthesis of native RNAs and AM Biotechnologies LLC (Dr. Xianbin Yang) for synthesis of the MS2-modified oligo. We would like to thank Drs. Muthiah Manoharan, Martin Maier, Klaus Charisse, Alexander Kel'in, Mark Schlegel, Vasant Jadhav, and Ivan Zlatev (Alnylam Pharmaceuticals), as well as Drs. David Cortez, Huzefa Dungrawala, F. Peter Guengerich, and Carl Sedgeman (Vanderbilt University) for helpful discussions. ITC data were acquired by Dr. Jia Ma at the Biophysical Analysis Laboratory, Purdue University, West Lafayette, IN. This work was supported by funding from Alnylam Pharmaceuticals and the National Institutes of Health (grant R01 GM071461).

Literature Cited

Abeydeera, N. D., Egli, M., Cox, N., Mercier, K., Conde, J. N., Pallan, P. S., ... Yang, X. (2016). Evoking picomolar binding in RNA by a single phosphorodithioate linkage. *Nucleic Acids Research*, *44*, 8052–8064. doi: 10.1093/nar/gkw725.

Alagia, A., Jorge, A. F., Aviñó, A., Cova, T. F. G. G., Crehuet, R., Grijalvo, S., ... Eritja, R. (2018). Exploring PAZ/3′-overhang interaction to improve siRNA specificity. A combined experimental and modeling study. *Chemical Science*, *9*, 2074–2086. doi: 10.1039/c8sc00010g.

Alves, C., & Cunha, C. (2012). Electrophoretic mobility shift assay: Analyzing protein-nucleic acid interactions. In S. Magdeldin (Ed.), *Gel electrophoresis - advanced techniques* (pp. 205–228). [Electronic resource]. Retrieved from *https://www.intechopen.com/books/gel-electrophoresis-advanced-techniques/electrophoretic-mobility-shift-assay-analyzing-protein-nucleic-acid-interactions*.

Andrus, A., & Kuimelis, R. G. (2001a). Polyacrylamide gel electrophoresis (PAGE) of synthetic nucleic acids. *Current Protocols in Nucleic Acid Chemistry*, *1*, 10.4.1–10.4.10. doi: 10.1002/0471142700.nc1004s01.

Andrus, A., & Kuimelis, R. G. (2001b), Overview of purification and analysis of synthetic nucleic acids. *Current Protocols in Nucleic Acid Chemistry*, *1*, 10.3.1–10.3.6. doi: 10.1002/0471142700.nc1003s01.

Andrus, A., & Kuimelis, R. G. (2001c). Cartridge methods for oligonucleotide purification. *Current Protocols in Nucleic Acid Chemistry*, *1*, 10.7.1–10.7.5. doi: 10.1002/0471142700.nc1007s01.

Barik, A., Mishra, A., & Bahadur, R. P. (2012). PRince: A web server for structural and physicochemical analysis of protein-RNA interface. *Nucleic Acids Research*, *40*, W440–W444. doi: 10.1093/nar/gks535.

Berman, H. M., Westbrook, J., Feng, Z., Gilliland, G., Bhat, T. N., Weissig, H., ... Bourne, P. E. (2000). The Protein Data Bank. *Nucleic Acids Research*, *28*, 235–242. doi: 10.1093/nar/28.1.235.

Chen, R. (2011). A general EMSA (gel-shift) protocol. *Bio-Protocol, Bio 101*, e24. doi: 10.21769/BioProtoc.24.

Cooper, M. A., & Whalen, C. (2005). Profiling molecular interactions using label-free acoustic screening. *Drug Discovery Today. Technologies*, *2*, 241–245. doi: 10.1016/j.ddtec.2005.08.014.

Crooke, S. T., Witztum, J. L., Bennett, C. F., & Baker, B. F. (2018). RNA-targeted therapeutics. *Cell Metabolism*, *227*, 714–739. doi: 10.1016/j.cmet.2018.03.004.

Cusack, S., Müller, C., Orengo, C., & Thornton, J. (Eds.) (2017). Protein-nucleic acid interactions. Catalysis and regulation. *Current Opinion in Structural Biology*, *47*, 1–176.

Elkayam, E., Kuhn, C. D., Tocilj, A., Haase, A. D., Greene, E. M., Hannon, G. J., & Joshua-Tor, L. (2012). The structure of human Argonaute-2 in complex with miR-20a. *Cell*, *150*, 100–110. doi: 10.1016/j.cell.2012.05.017.

Frank, F., Hauver, J., Sonenberg, N., & Bushan, N. (2012). *Arabidopsis* Argonaute MID domains use their nucleotide specificity loop to sort small RNAs. *EMBO Journal*, *31*, 3588–3595. doi: 10.1038/emboj.2012.204.

Fried, M. G. (1989). Measurement of protein-DNA interaction parameters by electrophoresis mobility shift assay. *Electrophoresis*, *10*, 366–376. doi: 10.1002/elps.1150100515.

Godber, B., Thompson, K. S., Rehak, M., Uludag, Y., Kelling, S., Sleptsov, A., ... Cooper, M. A. (2005). Direct quantification of analyte concentration by resonant acoustic profiling. *Clinical Chemistry*, *51*, 1962–1972. doi: 10.1373/clinchem.2005.053249.

Heffler, M. A., Walters, R. D., & Kugel, J. F. (2012). Using electrophoretic mobility shift assays to measure equilibrium dissociation constants: GAL4-p53 binding DNA as a model system. *Biochemistry and Molecular Biology Education*, *40*, 383–387. doi: 10.1002/bmb.20649.

Hellman, L. M., & Fried, M. G. (2007). Electrophoretic mobility shift assays (EMSA) for detecting protein-nucleic acid interactions. *Nature Protocols*, *2*, 1849–1861. doi: 10.1038/nprot.2007.249.

Jiang, X., & Egli, M. (2011). Use of chromophoric ligands to visually screen co-crystals of putative protein-nucleic acid complexes. *Current Protocols in Nucleic Acid Chemistry*, *46*, 7.15.1–7.15.8. doi: 10.1002/0471142700.nc0715s46.

Jing, M., & Bowser, M. (2011). Methods for measuring aptamer-protein equilibria: A review. *Analytica Chimica Acta*, *686*, 9–18. doi: 10.1016/j.aca.2010.10.032.

Kandeel, M., Al-Taher, A., Nakashima, R., Sakaguchi, T., Kandeel, A., Nagaya, Y., . . . Kitade, Y. (2014). Bioenergetics and gene silencing approaches for unraveling nucleotide recognition by the human EIF2C2/Ago2 PAZ domain. *PLoS One*, *9*, e94538. doi: 10.1371/journal.pone.0094538.

Long, S. B., Long, M. B., White, R. R., & Sullenger, B. A. (2008). Crystal structure of an RNA aptamer bound to thrombin. *RNA*, *14*, 2504–2512. doi: 10.1261/rna.1239308.

Lou, X., Egli, M., & Yang, X. (2016). Determining functional aptamer-protein interaction by biolayer interferometry. *Current Protocols in Nucleic Acid Chemistry*, *67*, 7.25.1–7.25.15. doi: 10.1002/cpnc.18.

Ma, J.-B., Ye, K., & Patel, D. J. (2004). Structural basis for overhang-specific small interfering RNA recognition by the PAZ domain. *Nature*, *429*, 318–322. doi: 10.1038/nature02519.

McDonnell, J. M. (2001). Surface plasmon resonance: Towards an understanding of the mechanisms of biological molecular recognition. *Current Opinion in Chemical Biology*, *5*, 572–577. doi: 10.1016/S1367-5931(00)00251-9.

Meister, G., Landthaler, M., Patkaniowska, A., Dorsett, Y., Teng, G., & Tuschl, T. (2004). Human Argonaute2 mediates RNA cleavage targeted by miRNAs and siRNAs. *Molecular Cell*, *15*, 185–197. doi: 10.1016/j.molcel.2004.07.007.

Mueller, A. M., Breitsprecher, D., Duhr, S., Baaske, P., Schubert, T., & Längst, G. (2017). MicroScale Thermophoresis: A rapid and precise method to quantify protein-nucleic acid interactions in solution. *Methods in Molecular Biology*, *1654*, 151–164. doi: 10.1007/978-1-4939-7231-9_10.

Pettersen, E. F., Goddard, T. D., Huang, C. C., Couch, G. S., Greenblatt, D. M., Meng, E. C., & Ferrin, T. E. (2004). UCSF Chimera–a visualization system for exploratory research and analysis. *Journal of Computational Chemistry*, *25*, 1605–1612. doi: 10.1002/jcc.20084.

Rozners, E., Pilch, D. S., & Egli, M. (2015). Calorimetry of nucleic acids. *Current Protocols in Nucleic Acid Chemistry*, *63*, 7.4.1–7.4.12. doi: 10.1002/0471142700.nc0704s63.

Schirle, N. T., & MacRae, I. J. (2012). The crystal structure of human Argonaute2. *Science*, *336*, 1037–1040. doi: 10.1126/science.1221551.

Schneider, C. A., Rasband, W. S., & Eliceiri, K. W. (2012). NIH Image to ImageJ: 25 years of image analysis. *Nature Methods*, *9*, 671–675. doi: 10.1038/nmeth.2089.

Shen, X., & Corey, D. R. (2018). Chemistry, mechanism and clinical status of antisense oligo-nucleotides and duplex RNAs. *Nucleic Acids Research*, *46*, 1584–1600. doi: 10.1093/nar/gkx1239.

Sheridan, C. (2017). With Alnylam's amyloidosis success, RNAi approval hopes soar. *Nature Biotechnology*, *35*, 995–997. doi: 10.1038/nbt1117-995.

Sheu-Gruttadauria, J., & MacRae, I. J. (2017). Structural foundations of RNA silencing by Argonaute. *Journal of Molecular Biology*, *429*, 2619–2639. doi: 10.1016/j.jmb.2017.07.018.

Sinha, N. D., & Jung, K. E. (2015). Analysis and purification of synthetic nucleic acids using HPLC. *Current Protocols in Nucleic Acid Chemistry*, *61*, 10.5.1–10.5.39. doi: 10.1002/0471142700.nc1005s61.

Teplova, M., Tereshko, V., Sanishvili, R., Joachimiak, A., Bushueva, T., Anderson, W. F., & Egli, M. (2000). The structure of the *yrdC* gene product from *E. coli* reveals a new fold and suggests a role in RNA-binding. *Protein Science*, *9*, 2557–2566. doi: 10.1110/ps.9.12.2557.

Tian, Y., Simanshu, D. K., Ma, J.-B., & Patel, D. J. (2011). Structural basis for piRNA 2′-O-methylated 3′-end recognition by Piwi PAZ (Piwi/Argonaute/Zwille) domains. *Proceedings of the National Academy of Sciences of the United States of America*, *108*, 903–910. doi: 10.1073/pnas.1017762108.

Tuma, R. S., Beaudet, M. P., Jin, X., Jones, L. J., Cheung, C. Y., Yue, S., & Singer, V. L. (1999). Characterization of SYBR Gold nucleic acid gel stain: A dye optimized for use with 300-nm ultraviolet transilluminators. *Analytical Biochemistry*, *268*, 278–288. doi: 10.1006/abio.1998.3067.

Watts, J. K., & Corey, D. R. (2012). Silencing disease genes in the laboratory and the clinic. *Journal of Pathology*, *226*, 365–379. doi:10.1002/path.2993.

Wilson, R. C., & Doudna, J. A. (2013). Molecular mechanisms of RNA interference. *Annual Review of Biophysics*, *42*, 217–239. doi: 10.1146/annurev-biophys-083012-130404.

Woodbury, C. P., Jr., & von Hippel, P. H. (1983). On the determination of deoxyribonucleic acid-protein interaction parameters using the nitrocellulose filter-binding assay.

Biochemistry, *22*, 4730–4737. doi: 10.1021/bi00289a018.

Yang, X., Fennewald, S., Luxon, B. A., Aronson, J., Herzog, N. K., & Gorenstein, D. G. (1999). Aptamers containing thymidine 3′-*O*-phosphorodithioates: Synthesis and binding to nuclear factor-κB. *Bioorganic & Medicinal Chemistry Letters*, *9*, 3357–3362. doi: 10.1016/S0960-894X(99)00600-9.

Yang, X. (2017). Solid-phase synthesis of RNA analogs containing phosphorodithioate linkages. *Current Protocols in Nucleic Acid Chemistry*, *70*, 4.77.1–4.77.13. doi: 10.1002/cpnc.40.